Applied Energy 256 (2019) 113841

Contents lists available at ScienceDirect

Applied Energy

journal homepage: www.elsevier.com/locate/apenergy

Accelerated fading recognition for lithium-ion batteries with Nickel-Cobalt-Manganese cathode using quantile regression method

Caiping Zhang[a], Yubin Wang[a,*], Yang Gao[a], Fang Wang[b,*], Biqiang Mu[c], Weige Zhang[a]

[a] National Active Distribution Network Technology Research Center (NANTEC), Beijing Jiaotong University, Beijing 100044, China
[b] Tianjin Key Laboratory of Evaluation Technology for Electric Vehicles, China Automotive Technology and Research Center Co., Ltd. (CATARC), Tianjin 300300, China
[c] Key Laboratory of Systems and Control of CAS, Institute of Systems Science, Academy of Mathematics and Systems Science, Chinese Academy of Sciences, Beijing 100190, China

HIGHLIGHTS

- Battery knee point recognition new method using quantile regression is proposed.
- The dynamic boundary determination method for the whole lifetime is developed.
- Recognition result is effective even if the input is disturbed.
- The proposed method has strong reliability and stability at different conditions.

ARTICLE INFO

Keywords:
Nickel-Cobalt-Manganese lithium-ion battery
Accelerated aging
Sudden degradation
Recognition
Quantile regression

ABSTRACT

The requirement for energy density of lithium-ion batteries becomes more urgent due to the rising demand for driving range of electric vehicles in recent years. Meanwhile, the performance stability of batteries with high energy densities tends to deteriorate, leading to accelerating degradation and safety issues. As a result, it is critical to explore the reasons that yield the sudden degradation and to recognize the degradation knee point of Nickel-Cobalt-Manganese batteries commonly used for electric vehicles. Existing results have disclosed that the lithium deposition of negative electrode dominates the sudden degradation of battery capacity. This paper extracts key parameters that characterize the aging status to facilitate knee point recognition in engineering practice. Furthermore, a novel method that integrates quantile regression and Monte Carlo simulation method to identify the accelerated fading knee point is introduced. The dynamic safety boundary determination method for the whole battery lifetime is proposed to update and monitor the safety zone. It is verified by experiments that the recognition results of capacity degradation knee point appear within 90–95% capacity range at 25 °C, 35 °C and 45 °C conditions, which can provide an early warning before the battery fails. Using the proposed method for recognizing the sudden degradation of capacity, recognition result is effective even if the input is disturbed and has strong reliability and stability under different conditions. It is helpful to promote the sustainable and stable development of the electric vehicles and improve advanced applied energy technologies.

1. Introduction

To conserve national energy and reduce emission, developing electric vehicles (EVs) has become a clear trend to deal with energy crisis and increasingly prominent environmental problems [1]. The most concerned quantities for EVs manufacturers and customers are the driving range and service life, which mainly depends on the energy density and remaining life of power batteries. Therefore, the requirement for the energy density of the lithium-ion battery is more rigorous, and its improvement has become the key to promoting the development of EVs [2].

Nickel-Cobalt-Manganese (NCM) lithium-ion batteries [3] are widely used in EVs due to the higher specific energy and longer cycle life [4] compared with other types of battery. However, NCM batteries with high energy density encounter sudden degradation [5] of battery capacities during usage, which not only greatly reduces the service life and durability of EVs, but also brings serious troubles for users when the EVs is running [6]. In 2017, General Motors Corporation (GM)

* Corresponding authors.
E-mail addresses: 18117024@bjtu.edu.cn (Y. Wang), wangfang2011@catarc.ac.cn (F. Wang).

https://doi.org/10.1016/j.apenergy.2019.113841
Received 24 March 2019; Received in revised form 9 August 2019; Accepted 1 September 2019
0306-2619/

suffered a remarkable economy loss from the recall of some Bolt EVs due to the failure of NCM lithium-ion batteries and the reason is that one of the batteries in the battery pack accelerated attenuation, which is also called the capacity “diving”. The voltage of suddenly decaying battery drops rapidly compared with other batteries. Once the battery management system detects that the voltage of any battery in the battery pack is under the limit, it will switch off the power system to avoid over-discharging the battery.

Numerous studies have confirmed that as the lithium-ion battery ages under normal operating conditions, the solid electrolyte interface (SEI) on the anode becomes thicker [7], and the available lithium ions are consumed [8], resulting in the linear degradation of the battery capacity with the number of cycles [9,10]. Meanwhile, there are some literatures report that the sudden degradation of battery capacity occurs, when the battery suffers from the abuse such as low temperature [11] and high charging cut-off voltage [12], even operates at the normal condition [13,14]. The capacity sudden degradation mechanism of the NCM lithium-ion battery under various operating conditions has been analyzed [15,16]. Zabala et al. [15] evaluated the aging mechanism by in-situ electrochemical measurements and ex-situ destructive physicochemical analysis, confirming that the abrupt decline of capacity is primarily affected by the growth of the SEI layer, resulting in localized lithium plating on the surface of the negative electrode (NE) during extended cycling. Ma et al. [16] systematically explored the effects of electrode material coating, electrolyte additive, upper cutoff voltage, electrolyte concentration, electrode thickness, and graphite type on the sudden degradation of battery capacity, and found that impedance growth is the main cause. It can be concluded that the essential cause of sudden degradation is mainly the lithium deposition of NE, which make the porosity of the electrode to decrease and the SEI layer to grow rapidly. The battery system consists of hundreds or even thousands of lithium-ion batteries connected in series and parallel. Once the sudden degradation occurs, the performance of the battery drops sharply in a short period of time. Furthermore, it is also observed that the batteries begin to expand noticeably since side reactions occur inside the battery, which results in electrolyte decomposition to generate a large amount of gas. This may lead to battery failure and affect the normal operation of the system. In severe cases, the deposited lithium pierces the separator to cause the internal short circuit, and the battery system fires and explodes. This not only causes huge economic losses, but also jeopardizes life safety, greatly restricting the development of energy conversion and conservation technologies.

Real cases of the battery sudden degradation and related mechanism research work have forced us to pay attention to the knee point recognition of sudden degradation for battery capacity. Recognizing the sudden degradation of capacity, it is not only possible to judge the fading trajectory of the battery to play an early warning role, but also to provide guide for replacing the sudden decay battery in time, thereby effectively reducing the safety hazard and improving the performance of the battery pack. It is helpful to promote the sustainable and stable development of the EVs and improve advanced applied energy technologies.

There are few researches on methods for identifying capacity accelerated fading knee point of NCM lithium-ion batteries, but most studies focus on remaining useful life (RUL) prediction and state of health (SOH) estimation. The termination condition of the battery life is generally considered as when the battery capacity declines to 70%-80% of the initial rated capacity or the internal resistance increases to 160%-200% of the initial value. The remaining life can be defined as the length of time from now to the moment when the battery termination condition is reached [17]. The remaining life prediction methods are divided into two categories: model-driven methods and data-driven methods. The fundamental difference between model-based and data-driven methods is whether there is prior knowledge. This prior knowledge may be an empirical model or a physical model that considers the aging mechanism. Model-driven methods have clarified mathematical expression of the battery capacity or internal resistance with respect to the number of cycles before the prediction. Data-driven methods have no well-defined mathematical expression, using a large amount of data to construct an approximate relationship to imitate the real situation.

Implementing the model-driven method has two fold. One relies on the laboratory data under some specific conditions to summarize the evolution law of battery aging, and further establishes empirical models. Another implementation considers the aging mechanism. Ramadesigan et al. [18] and Safari et al. [19] observed chemical reactions and structural changes inside the battery and constructed physicochemical models of battery decay through thermodynamic and kinetic equations. This approach provides a deeper understanding of the decay mechanism of battery capacity, and yields the model having higher prediction accuracy under specific operating conditions than other empirical models. The key of the method is to determine parameters in the model in terms of the measured data when the model structure is determined. A large number of parameter estimation methods such as particle filtering (PF), Kalman filtering (KF), and unscented particle filtering (UPF) have been proposed. Zhang et al. [20] found that the lithium-ion battery capacity declines exponentially and developed a prediction method based on exponential model and PF. Guha et al. [21] combined the double exponential capacity decay model with the fourth-order polynomial internal resistance growth model for the remaining life prediction. Zhang et al. [22] proposed an improved PF algorithm using linear optimization integrated resampling UPF to improve prediction accuracy. In Ref. [23], Markov Chain Monte Carlo (MCMC) methods were used to improve the UPF and establish an empirical capacity decay mode. In Ref. [24], Bayesian network theory based model was explored, model parameters were inferred from statistical methods through prior distribution [25,26]. Yang et al. [27] extracted four feature parameters that can well reflect the aging status of batteries as inputs to Gaussian Process Regression (GPR) models. In Ref. [28], the proposed life prediction methods based on multi-hidden nonlinear drift Brownian motion were verified to be more accurate than the PF and Bayesian methods. Although the model-driven methods have a clear expression, it brings unavoidable model prediction error due to uncertainty of model parameters.

Data-driven methods rely on a large amount of existing data rather than a preset model to fit the data with many simple models, finding one or a combination of a set of models that extremely approximate to the real situation. Although the obtained model may have a certain deviation from the real model, in terms of the prediction result, it is sufficiently close to the accurate model within the error tolerance. Data-driven methods can either directly deal with the original data or convert the original data into some features having a certain relationship with predicted values by means of mathematical or signal processing method for machine learning. Li et al. [29] proposed a deep convolutional neural network (DCNN) that uses measured values for learning prediction without known prior distribution. Patil et al. [30] extracted the key feature to construct database from the aging data of lithium-ion battery under different working conditions. Further, an initial estimation was performed to narrow the range of prediction results by using support vector machine (SVM) based classification technique, laying the foundation for accurate life prediction by regression. Wei et al. [31] extracted the time and capacity of the constant voltage (CV) charging process as feature parameters, and established the state space formula based on support vector regression (SVR) that simulates the battery capacity degradation. In Ref. [32], it was found that the capacity of Li $(NiCoAl)O_2$ or $LiCoO_2$ battery showed a downward convex trend with the cycle numbers. In this case, the feature converted from battery capacity via Box-Cox transformation had a clear linear relationship with cycle numbers. Cai et al. [33] processed the row data based on wavelet transform to build the cross D-Markov machine learning model. In Ref. [34], the charging curve was translated, rotated and scaled based on dynamic space time warping (DSTW), recognizing the relationship between the judgement curve and reference curve to predict the degradation state. Data-driven methods yield a slightly different model from the real world, but it is sufficient to guide practice. More importantly, data-driven methods can be implemented more easily with the development of computer technology.

All of the aforementioned methods aimed to RUL prediction and SOH estimation, which indicates the remaining life and health status of the battery at the current moment. However, the operating environment of batteries is rather complicated in practical application scenarios. And capacity fading process of batteries is affected by many factors, such as temperature, current, and depth of discharge, which make the accurate prediction of the RUL difficult. Moreover, when a battery starts the accelerated attenuation, the remaining life is less than 20% of the entire life and the consistency difference of the battery pack is great. Under these circumstances, RUL prediction and SOH estimation have estimation errors and uncertainty in the prediction results, it has difficulty in determining whether appearing sudden degradation at current state. In order to avoid the troubles and safety risks mentioned earlier, a method that can quickly and accurately identify the capacity accelerated fading knee point is particularly indispensable.

Based on the investigation of battery degradation mechanisms, this paper extracts the parameters that characterize the state of aging and develops a method integrating quantile regression and Monte Carlo simulation to identify the capacity accelerated fading knee point. The rest of the article will be presented in the following. Section 2 introduces the battery cycle life test matrix. Section 3 depicts the battery degradation mechanism and corresponding characterization parameter extraction. Section 4 presents the principle and implementation of the accelerated fading knee point recognition algorithm. Section 5 demonstrates the identification results and effectiveness analysis of the developed method. Finally, main findings are summarized in Section 6.

2. Battery cycle life test matrix

Cycle life tests under different operating conditions are carried out to study the accelerated fading mechanism and identification method of NCM lithium-ion batteries. The selected battery is a commercial 36Ah NCM lithium-ion battery with the graphite anode. The working voltage ranges from 2.8 V to 4.2 V. Experiments are performed on the platform consisting of a Maccor Battery Testing System, a PC host computer and a thermostat. The test scheme is the constant current-constant voltage (CC-CV) charge and constant current (CC) discharge. According to the ambient temperature and current rate, the experimental matrix is compartmentalized into four groups, which is recorded in Table 1.

The capacity fading curves under different temperatures are illustrated in Fig. 1. It can be seen that battery capacities under all kinds of cyclic conditions show the accelerated decline stage. The capacities decay slowly and exhibit approximately linear characteristics as the cycle numbers increase at the initial stage. Unexpectedly, the capacity deterioration suddenly accelerates at the end of cycling experiments. When accelerating recession occurs, the sample batteries under the same operating condition have almost identical cycle numbers. For batteries under different temperatures, the cycle numbers show a tremendous difference at the accelerated knee point, which are around 500 cycles at the condition of 25 °C and 1 C charge-1 C discharge

Table 1
Cycle life experimental matrix of NCM lithium-ion batteries under different temperature and rate conditions.

Battery number	Temperature (°C)	Rate (charge-discharge)
1#, 2#	25	1 C–1 C
3#, 4#	35	1 C–1 C
5#, 6#	45	1 C –1 C
7#, 8#	25	0.5 C–1 C

(25 °C@1 C–1 C) and 45 °C and 1 C charge-1 C discharge (45 °C@1 C–1 C), 800 cycles at the condition of 35 °C and 1 C charge-1 C discharge (35 °C@1 C–1 C). Furthermore, as the aging accelerates, it is also observed from the experiment that the batteries begin to expand noticeably since side reactions occur inside the battery, which results in electrolyte decomposition to generate gas. The accelerated capacity degradation and drastic appearance change undoubtedly bring great troubles and safety risks to the use of NCM lithium ion batteries, which makes the recession knee point identification extremely urgent.

3. Capacity fading mechanism and characteristic parameter extraction

In the interest of identifying the moment when the sudden battery degradation occurs, acquiring the available capacity of the battery is necessary. However, since the battery can hardly be discharged continuously to 0% State-of-Charge (SOC) under practical applications, the true value of the capacity is difficult to obtain and can only be estimated in real time. There is an error in using the real-time capacity estimation method, resulting in inaccurate knee point recognition results. Therefore, finding some characteristic parameters that change drastically after battery sudden degradation to replace the capacity for knee point identification is indispensable. Meanwhile, existing results have disclosed that the lithium deposition of NE dominates the sudden degradation of battery capacity. For the lithium deposition on the NE, the battery exhibits the abrupt loss of negative active material and available lithium ions. In Ref. [35], a multi-index characterization system revealing the aging state of lithium-ion battery was established by extracting key features from the Increment Capacity (IC) curve at the current rate of 0.05 C. IC curve is derived from the charging curve (Q-V curve). Key features of the IC curve are able to respectively reflect the loss of positive and negative active materials, and available lithium ions, in particular some key features can even be obtained through a partial charging curve, which is more convenient to be implemented in engineering practice. Combined with the capacity sudden degradation mechanism and indicator system of the IC curve, characteristic parameters for the knee point identification are inferred.

For the battery that cycles at 35 °C@1 C–1 C condition, the IC curve at the current rate of 0.05 C is shown in Fig. 2a. The IC curve is obviously composed of three regions shaped like mountains, which are labeled as $NE_{peak\ I}$, $NE_{peak\ II}$ and $NE_{peak\ III}$. The voltage points that distinguish different regions are determined by deriving the IC curve. The minimum voltage point that the second derivative of the IC curve is zero is taken as the starting point of $NE_{peak\ I}$. The first local minimum voltage value of the IC curve is regarded as the separation point between $NE_{peak\ I}$ and $NE_{peak\ II}$, and the second local minimum voltage value of the IC curve is considered as the separation point between $NE_{peak\ II}$ and $NE_{peak\ III}$. The charging cutoff voltage is used as the end point of $NE_{peak\ III}$. Each region has two key features: the area and height of the region. Thus, a total of six features exist: the area and height of the $NE_{peak\ I}$, $NE_{peak\ II}$, and $NE_{peak\ III}$. In our previous papers [35,36], the relationship between IC curve characteristics and battery capacity degradation has been studied and verified by experimental data. It can be roughly maintained that the attenuation of the $NE_{peak\ I}$ and $NE_{peak\ III}$ region represent the loss of the negative active material and available lithium ions, respectively. And the attenuation of the $NE_{peak\ II}$ region simultaneously involves the loss of the two materials. In specific, the area of $NE_{peak\ III}$ and the height of $NE_{peak\ II}$ reflect the loss of available lithium ions, and the area of $NE_{peak\ I}$ and $NE_{peak\ II}$ can be used to characterize the loss of the negative active material. Since the amount of available lithium ions and negative active material are suddenly reduced when the battery deterioration is accelerated, the attenuation rate of these four parameters sharply increases. The above IC characteristic parameters are extracted from the charging data at the current of 0.05 C. However, the charging current rate of EVs is much higher than 0.05 C, and the obtained IC curve is somewhat different

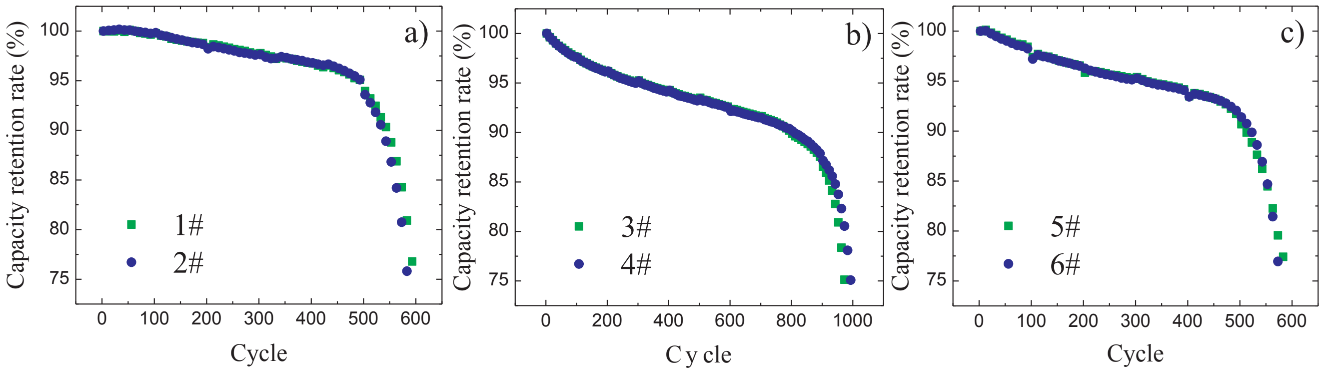

Fig. 1. Capacity retention rate decay curves of NCM lithium-ion batteries under 25 °C@1 C–1 C, 35 °C@1 C–1 C and 45 °C@1 C–1 C conditions (a) Capacity retention rate decay curve at 25 °C@1 C–1 C (b) Capacity retention rate decay curve at 35 °C@1 C–1 C (c) Capacity retention rate decay curve at 45 °C@1 C–1 C.

from the IC curve at the current of 0.05 C, so that partial IC characteristics become quite inconspicuous. Therefore, it is necessary to expand the charging current to a relatively large rate based on the original IC curve indexing system, so as to determine the specific characteristic parameters for identifying the accelerated knee point.

When the current rate is increased to 1 C, the evolution of the IC curve of the battery that cycles at 35 °C@1 C–1 C condition is reported in Fig. 2b. Compared with the IC curve at the current of 0.05 C, the distinct disparity is that the valley point between the $NE_{peak\ II}$ and the $NE_{peak\ III}$ disappears after the current rate is raised, resulting in the overlap of the two regions. Only by finding a way to separate the two regions, the relevant parameters can be extracted. The IC curve drops sharply after passing the peak of $NE_{peak\ II}$ and then enters a platform area gently ($NE_{peak\ III}$). The corresponding entry voltage hardly varies with battery aging, for the sake of simplicity, the IC curve at a high current rate is divided into two regions of $NE_{peak\ II}$ and $NE_{peak\ III}$ at a fixed voltage point. There is still a distinct minimum point between $NE_{peak\ I}$ and $NE_{peak\ II}$ after battery aging, which is used to separate $NE_{peak\ I}$ from $NE_{peak\ II}$. During the actual use of the battery, the starting SOC of each charge process is not exactly same. The area of the IC curve is so trivial that it can be ignored at the initial charging stage, so the voltage at which the IC curve rises rapidly is selected as the starting point when calculating the area of $NE_{peak\ I}$. In addition, due to the presence of ohmic and polarization voltages, charging to the cut-off voltage at a high rate does not fill the battery and the $NE_{peak\ III}$ region no longer retains physical properties, so the area of $NE_{peak\ III}$ is not suitable as a characteristic parameter. In general, during the large rate charging process, three IC features are extracted to characterize the aging status, namely, the areas of $NE_{peak\ I}$ and $NE_{peak\ II}$, and the height of $NE_{peak\ II}$. As seen from Fig. 2b that the three features of the IC curve show a significant difference before and after capacity sudden degradation. At the normal capacity degradation stage, the battery has experienced 800 cycles, but the features of the IC curve hardly attenuate. After that, the battery has only experienced 170 cycles, and the IC curve shows a very significant change. This phenomenon under the 35 °C@1 C–1 C condition is very promising for the knee point identification of the battery sudden degradation. Nevertheless, the ambient temperature and current rate experienced by batteries in real applications are complex and variable. Under other conditions, whether there is such a promising phenomenon needs further verification.

Fig. 3 shows the evolution of three IC parameters with cycle numbers under different conditions, which displays a similar behavior of capacity decay. Moreover, before the sudden degradation, the area of $NE_{peak\ I}$ hardly attenuates but the height of $NE_{peak\ II}$ presents the slight attenuation. It can be seen that the attenuation mechanism of the battery at this stage is slight lithium ion loss, because the area of $NE_{peak\ I}$ is affected by the loss of the negative active material, and the height of $NE_{peak\ II}$ is affected by the loss of lithium ions. The demarcation point between the $NE_{peak\ II}$ and $NE_{peak\ III}$ regions will shift as the battery ages. Affected by the fixed voltage division method, the area of the $NE_{peak\ II}$ is inevitably interfered by the $NE_{peak\ III}$, and the latter also reflects the loss of lithium ions, so the area of the $NE_{peak\ II}$ slightly attenuates. The capacity and three parameters simultaneously began to accelerate the decline, which verifies that the three parameters have the ability to identify the knee point of the battery sudden degradation under different operating conditions. In addition, it can be seen from Fig. 3 that the knee point appears in the 90%-95% capacity range. This is because the experimental data is obtained from the laboratory and only the 25 °C, 35 °C and 45 °C conditions of a type of battery are introduced, and the sample batteries are fully charged and discharged. However,

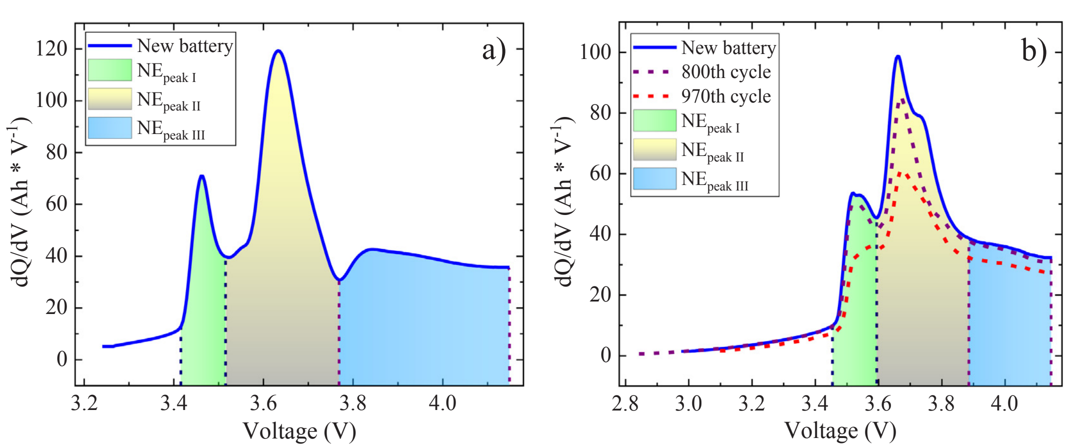

Fig. 2. The IC curve and region division at the charging current rate of 0.05 C and 1 C for the battery cycled under 35 °C@1 C–1 C condition (a) The IC curve and region division of charging at the current of 0.05 C (b) The IC curve and region division of charging at the current of 1 C.

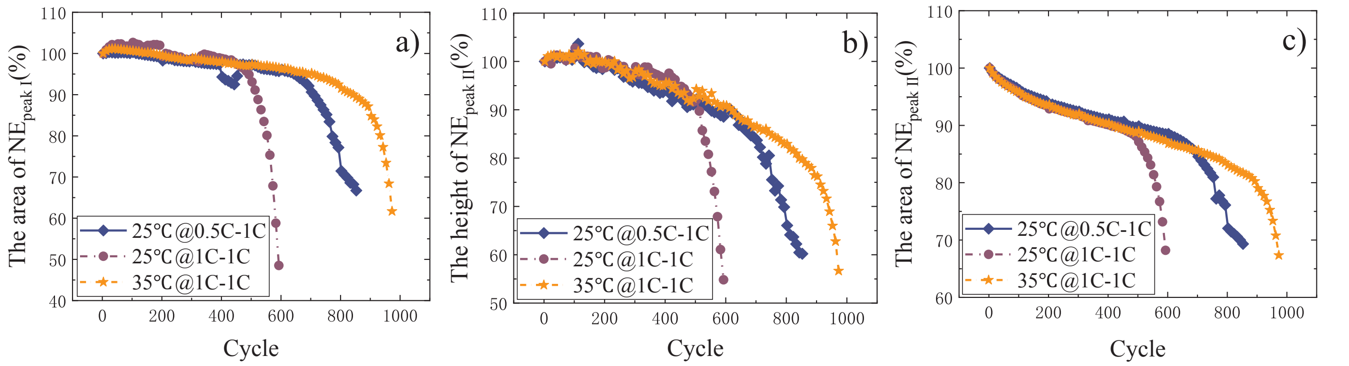

Fig. 3. The evolution of three IC parameters with cycle numbers under 25 °C@0.5 C–1 C, 25 °C@1 C–1 C and 35 °C@1 C–1 C conditions, including the area of $NE_{peak\ I}$ and $NE_{peak\ II}$, and the height of $NE_{peak\ II}$ (a) The evolution of the area of $NE_{peak\ I}$ (b) The evolution of the height of $NE_{peak\ II}$ (c) The evolution of the area of $NE_{peak\ II}$.

the temperature, charge/discharge rate and depth of discharge are varying under application operating conditions. The reasons of battery sudden degradation are quite complicated resulted from the electrode material, the electrolyte additive, the manufacturing process, and so on. The lab test results can not represent that of the real condition. Therefore, the law of the knee point appears within 90–95% capacity range cannot be directly applied to other conditions. Our approach is designed to provide a general method for identifying the knee point of capacity decline, it is therefore necessary to identify it in real-time. In order to facilitate online capacity acceleration degradation identification, it is not desirable to store a large amount of charging data and perform complicated calculations. The height of $NE_{peak\ II}$ is an instantaneous variable and can be obtained by finding the maximum value on the IC curve, which is easier to implement than the other two parameters. Ultimately, the height of $NE_{peak\ II}$ is applied in the paper to the accelerated degradation identification.

4. Accelerated degradation recognition algorithm

The linear regression model estimates the conditional mean of the response variable given certain values of the predictor variables and the ordinary least squares estimation (OLSE) is the standard estimation method. If the residuals satisfy independence, normality, and homoscedasticity, the OLSE is the unbiased least variance estimate. In practical application scenarios, the measured data is difficult to meet such restricted assumptions. Instead, quantile regression does not require strong assumptions on the error term and can accurately model the effect of the explanatory variables on the range and conditional distribution of the interpreted variable [37]. Regression with various quantiles can get different expressions, which is more comprehensive in portraying the interpreted variables than OLSE [38]. Therefore, for the accelerated fading knee point identification of battery capacity, quantile regression has the potential to perform more reasonably and effectively than the OLSE.

4.1. Quantile regression principle

Suppose the distribution function of the random variable X is:

$$F(x) = P(X \le x) \tag{1}$$

The τ quantile can be defined as:

$$Q_\tau(X) = inf\{x \in R\colon F(x) \ge \tau\}(0 < \tau < 1) \tag{2}$$

A random vector (X, Y), where the distribution function of Y given $X = x$ is:

$$F_{Y|X=x}(y|x) \tag{3}$$

The τ conditional quantile of the conditional random variable $Y|X = x$ is defined as:

$$Q_\tau(Y|X = x) = inf\{y \in R\colon F(y|x) \ge \tau\}(0 < \tau < 1) \tag{4}$$

Regression analysis is to minimize the distance between the sample value and the fitted value. Suppose we have a sample sequence: $\{(X_i, Y_i), (i = 1, \cdots, n)\}$

Then the quantile regression is to minimize the sum of the absolute values of the weighted errors, namely:

$$\min_{\xi \subset R} \sum_{i=1}^{n} \rho_\tau(y_i - \xi) \tag{5}$$

where $\rho_\tau(u) = u(\tau - \mathrm{I}(u < 0))$ is the loss function and $I(Z)$ is the indicator function on the set Z.

When the quantile is 0.5, it is the median regression. Both the loss functions of least squares regression and median regression are symmetric, while the loss function of quantile regression is asymmetric. Actually, it consists of two rays from the origin that are located in the first and second quadrants respectively. Quantile regression is an extension of the least squares method based on the classical conditional mean model. The global model is estimated by multiple quantile functions, and the absolute value of the residual is minimized over asymmetric weights.

If $\hat{y}_{(\tau)i}$ is used to represent the quantile estimator of y_i, then $\sum_{i=1}^{n} \rho_\tau\ |y_i - \alpha|$ has a minimum value for any value α only when $\alpha = \hat{y}_{(\tau)i}$, where:

$$\sum_{i=1}^{n} \rho_\tau\ |y_i - \alpha| = -\sum_{i:y_i<\alpha} (1-\tau)(y_i - \alpha) + \sum_{i:y_i \ge \alpha} \tau(y_i - \alpha) \tag{6}$$

Assume that the response variable Y is linearly represented by the matrix X consisting of k explanatory variables and the coefficient β as a linear regression model:

$$y_i = X\beta + u_i \tag{7}$$

Then the estimated value of the coefficient of the τ quantile regression equation is given by:

$$\hat{\beta}_{(\tau)} = arg\min_{\beta \subset R^k}\left(-\sum_{i:\hat{u}_{(\tau)i}<0} (1-\tau)\hat{u}_{(\tau)i} + \sum_{i:\hat{u}_{(\tau)i}\ge 0} \tau\hat{u}_{(\tau)i}\right) \tag{8}$$

$$\hat{\beta}_{(\tau)} = arg\min_{\beta \subset R^k}\left(-\sum_{i:y_i<X\hat{\beta}_{(\tau)}} (1-\tau)(y_i - X\hat{\beta}_{(\tau)}) + \sum_{i:y_i \ge X\hat{\beta}_{(\tau)}} \tau(y_i - X\hat{\beta}_{(\tau)})\right) \tag{9}$$

where y_i is the actual data, $\hat{u}_{(\tau)i}$ represents the residual corresponding to the τ quantile regression equation. The expression of the τ quantile regression equation is:

$$\hat{y}_{(\tau)i} = X\hat{\beta}_{(\tau)} \tag{10}$$

Once the estimated quantile regression equation is obtained, the linear relationship between battery capacity and cycling number can be established. More quantile regression equations obtained, more comprehensive understanding of the conditional distribution for explanatory variables. The distribution of explanatory variables is asymmetric when the median regression line is significantly different from the mean regression line. The distribution of response variable is left-biased while the upper quantile regression line is close to the lower quantile regression line, and right-biased otherwise. The coefficient disparity of the regression function is evident and the effect of explanatory variables on the response variable is notably distinct in multiple quantiles.

4.2. Implementation

Lithium-ion batteries experience many kinds of failure modes such as the pole breakage, internal short circuit, battery perforation, deformation, and bulging. Nevertheless, it is difficult to detect the aforementioned failure modes directly since only external parameters including battery terminal voltage, current and temperature can be monitored in real time by employing battery management system (BMS), which does not have a consistent correspondence reflecting the internal failure properties of batteries. Battery failures are usually accompanied by anomalies and reflected in recorded data. This provides a potential for exploring battery safety and fault warning based on the external parameters information of batteries. For example, the battery begins to exhibit bulging when the height of $NE_{peak\ II}$ shows a significant knee point. Theoretically, the knee point is the intersection of two straight lines with different slopes, which can be identified according to the sudden change of the slope. Due to the interference of data acquisition and processing error, the slope of the line connected by adjacent cycles is inevitably abrupt, making the method of finding the slope change point difficult to apply. To this end, the paper learns a straight line as the baseline from experimental data and determines the boundary on both sides of the baseline to establish a strip-shaped safety zone. Thus the point beyond the safety zone is considered to be the knee point of the curve. Taking the accelerated fading knee point as the demarcation point, the full life cycle of batteries can be divided into two stages, which are defined as the safe operation stage and the fault operation stage respectively. Battery safety zone and operation stage division diagram is shown in Fig. 4, where "○" represents the knee point in the process of fading. The cycle before the knee point is the safe operation stage, and the subsequent cycle is the fault operation stage. The region within the two boundaries of the baseline is defined as the safety zone, which is determined by the baseline, the distance d_u from the baseline to the upper boundary, and the distance d_l from the baseline to the lower boundary. The battery capacity starts accelerating decline when the height of $NE_{peak\ II}$ exceeds the safety zone.

After clarifying the definition of the safety zone, the difficulty in identifying the knee point is how to fit the baseline and confirm the boundaries of the strip-shaped safety zone. To resolve the above issue, first of all, the quantile regression algorithm is used to fit the height of the $NE_{peak\ II}$ from the decile of 0.5–0.9, and five regression lines are obtained. The regression algorithm should grant higher weight to the previous data since the data of the safe operation stage is linearly degraded. The regression lines with the decile greater than 0.5 quantiles are therefore selected. Therein, a line that minimizes the dispersion of the residual between the estimated value and the true value is chosen as the baseline of the strip-shaped safety zone. Followed by, the values of d_u and d_l are determined by performing the Monte Carlo simulation on the residual so that the probability of the height of the $NE_{peak\ II}$ being within the safety zone is 95%. Thus the boundaries of the safety zone can be confirmed. Note that the residuals used for the Monte Carlo simulation are determined by their quartile and interquartile range because the height of the $NE_{peak\ II}$ is easily interfered by the outliers during the acquisition process. Thus only the data that satisfies the following conditions:

$$Q_1 - 1.5 * IQR \le x \le Q_3 + 1.5 * IQR \tag{11}$$

is chosen for the Monte Carlo simulation, where x is the residual between the estimated value and the true value, Q_1 and Q_3 are the quarter quantile and third-quarter quantile of the residual, respectively, and IQR is the interquartile range of the residual. Residuals outside this range are regarded as outliers based on quartile and interquartile range. It follows that the quartile is more resistant to disturbances since up to 25% of the data can be distributed as far as possible without greatly disturbing the quartile [39]. Therefore, the outliers will not affect the criterion and the corresponding results on identifying outliers are more robust.

Based on the safety boundaries determination, we can find that the probability of the height of $NE_{peak\ II}$ exceeding the safety zone is 5%. It is inferred that the probability for four consecutive cycles exceeding the safety zone is less than 0.01%, which can be considered as an event with a very low probability. The last cycle can then be determined as the knee point in the process of capacity fading. In addition, the cycle numbers in the safe operation stage of the battery are difficult to identify due to effects of battery temperature, charge/discharge rate and depth of discharge. It is necessary to continuously update the safety zone with increasing cycle numbers during the whole life of the battery, enhancing the adaptability of the algorithm to different conditions.

The flow chart of the capacity accelerated fading knee point identification of NCM lithium-ion batteries is shown in Fig. 5, which is divided into four steps: (1) feature parameter extraction, (2) safety zone establishment, (3) safety zone update, and (4) accelerated knee point identification. By extending the multi-index aging characterization system to the large-rate charging field and combining with the mechanism of sudden capacity decline, the characteristic parameters for the accelerated knee point identification are extracted. The ribbon safety zone consisting of baseline and bandwidth are finally determined by integrating quantile regression with Monte Carlo simulation. The real-time update of the safety zone can improve the adaptability of the proposed method under various conditions. In a word, the identification of the accelerated recession knee point under different working conditions is implemented.

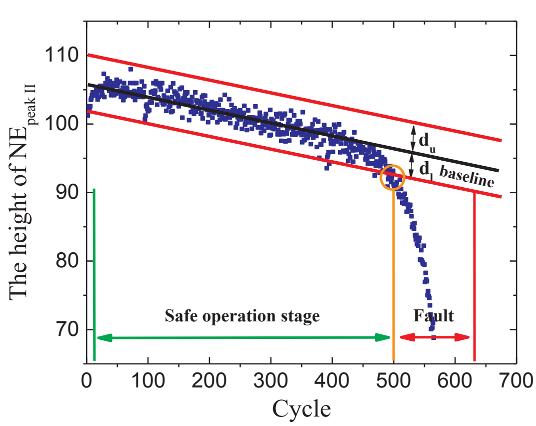

Fig. 4. Safety zone and operation stage division diagram of NCM lithium-ion battery.

5. Results and discussion

Fig. 1 shows that the capacity attenuation of the two batteries is consistent at the same temperature. Therefore, one of batteries is selected to perform battery capacity accelerated decay knee point identification under each operating condition based on the proposed method. First of all, the IC curve is derived from the charging curve (Q-V curve) of the selected battery. The height of $NE_{peak\ II}$ is extracted from the IC curve to obtain a straight line as the baseline using quantile regression method, and the bandwidths are determined by performing the

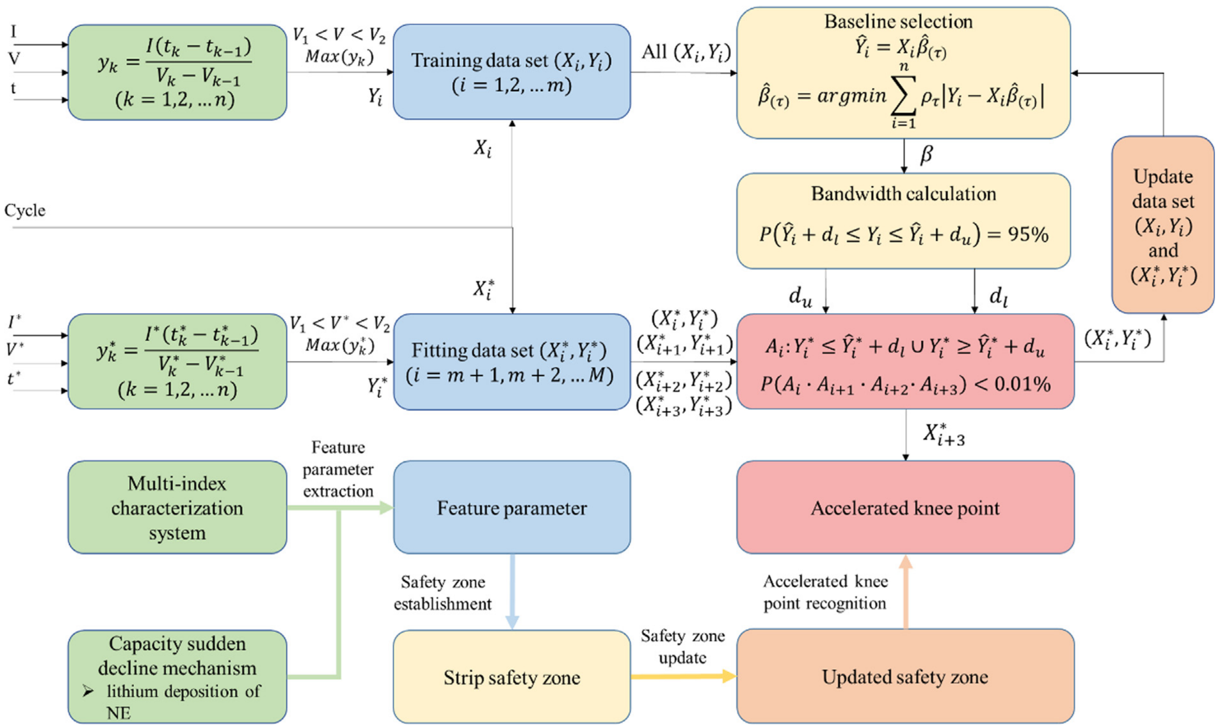

Fig. 5. The flow chart for the capacity accelerated fading knee point identification of NCM lithium-ion batteries.

Monte Carlo simulation so that the probability of the data being within the safety zone is 95%. After that, if there are four consecutive cycles beyond the safety zone, the last cycle can then be determined as the knee point in the process of capacity fading. In addition, the safety zone is continuously updated with increasing cycle numbers during the whole life of the battery.

The safety zone and the capacity accelerated fading knee point at 25 °C@1 C–1 C, 35 °C@1 C–1 C and 45 °C@1 C–1 C conditions are shown in Fig. 6, and the cycle numbers corresponding to accelerated knee points are 487, 774 and 504, respectively. At present, there is no clear mathematical definition of the knee point. The calculation of the knee point is only by judging whether the change of the slope connected by each adjacent cycles exceeds the threshold, and the threshold is an empirical value and is not fixed. Therefore, there is no reference value for the knee point. It is verified by experiments that the recognition results of capacity degradation knee point using proposed method appear within 90%-95% capacity range, which can provide an early warning before the battery fails. Although the distribution of the height of $NE_{peak\ II}$ under the considered three conditions has different characteristics, which is concentrated in Fig. 6a and b, and is seriously disturbed by outliers in Fig. 6a, and while is more scattered in Fig. 6c. From the perspective of results, the proposed method is effective to different data distribution conditions by adaptively adjusting the baseline and computing bandwidth. In more detail, the key procedures of the proposed method are the establishment and update of the safety zone, which determines the effectiveness of the method and require further discussion.

As seen from the establishment of the safety zone in terms of the identification results above, the baseline selection and calculation of the bandwidths d_u and d_l are critical factors. Apart from the proposed method, there are two traditional methods that can be adopted as candidates. One method applied the same selection criteria as the proposed method to determine the baseline, as discussed in Section 4. The extreme values of regression residuals were employed to calculate the d_u and d_l by Monte Carlo simulation. The height of $NE_{peak\ II}$ is not processed and original information is utilized. The other method is to perform a normality test on the residuals between the quantile regression value and true value. The regression line that the residuals pass the normality test is chosen as the baseline and the "u ± 3σ" distance of the residuals is applied to calculate the d_u and d_l. Once the safety

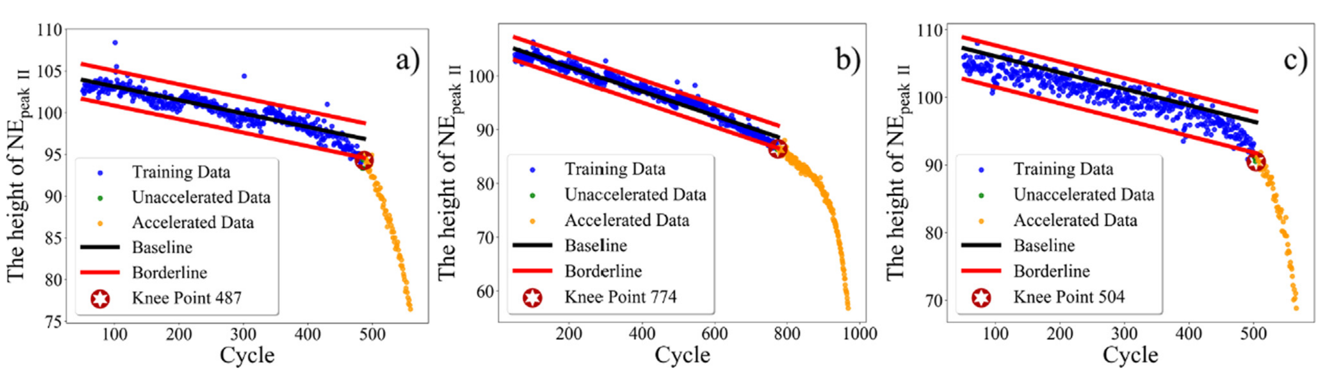

Fig. 6. The safety zone and the recognition results of capacity accelerated decay knee point using proposed method for NCM lithium-ion batteries under 25 °C@1 C–1 C, 35 °C@1 C–1 C and 45 °C@1 C–1 C conditions (a) The safety zone and the recognition result at 25 °C@1 C–1 C (b) The safety zone and the recognition result at 35 °C@1 C–1 C (c) The safety zone and the recognition result at 45 °C@1 C–1 C.

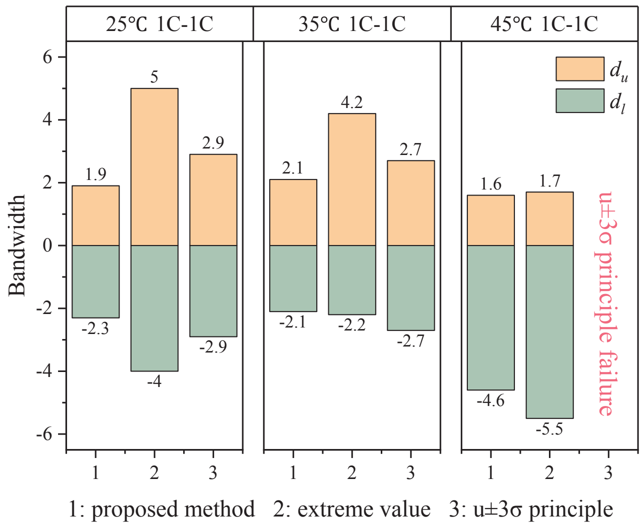

Fig. 7. The Comparison of safety zone bandwidths established through proposed method, extreme value and "μ + 3σ" principle.

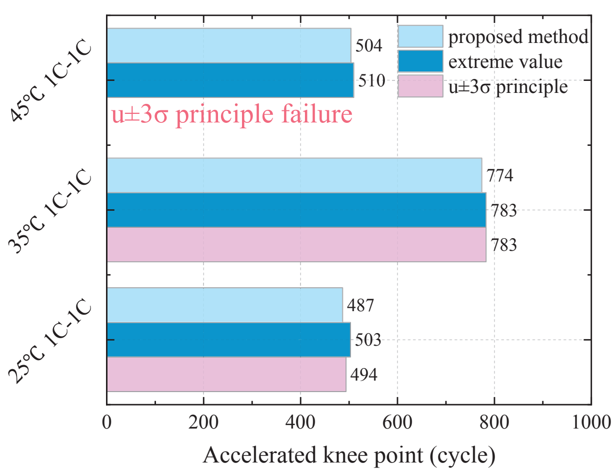

Fig. 8. The impact of the safety zone establishment method on the identification results of accelerated knee point.

boundary is successfully established using the three methods, the probability that the height of $NE_{peak\ II}$ exceeds the safety zone can be clearly defined to facilitate the identification of the acceleration knee point. Their safety zone bandwidths and identification results at 25 °C@1 C–1 C, 35 °C@1 C–1 C and 45 °C@1 C–1 C conditions are comparatively shown in Figs. 7 and 8. For the method of establishing the safe boundary with extreme values, the cycle numbers of accelerated decay knee points are 503, 783 and 510, respectively. Compared with the proposed method, the identification result of the accelerated recession point is delayed, especially for the data distribution with severe interference from outliers, resulting in a broader safety zone. It is highly sensitive to anomalous data for bandwidth calculations, increasing the risk of security incidents. With regard to the method in virtue of the "u ± 3σ" principle, the cycle numbers of accelerated recession points at 25 °C@1 C–1 C and 35 °C@1 C–1 C conditions are 494 and 783 respectively, slightly behind the proposed method. Unfortunately, under the condition of 45 °C@1 C–1 C, the data distribution is relatively dispersed, the accelerated decay point could not be identified. Although the "3σ" principle of normal distribution has the theoretical basis of hypothesis testing, the requirements for real data are too strict to satisfy. Once the residual of the regression line cannot pass the normal test, the "3σ" standard cannot be used to establish the safety zone for accelerated decay knee point recognition, leading to the failure of method and tremendous safety risk. To sum up, the proposed method can prominently improve the robustness and reliability of the safety zone establishment in comparison with the two traditional methods above.

In addition to the safety zone establishment, another key process affecting the recognition effect is the update of the safety zone. Despite cycle numbers in the safe operation stage are unequal under different operating conditions, the height of $NE_{peak\ II}$ for all batteries exhibit linearly decaying characteristics, making it unnecessary to continuously update the safety zone after it is initialed. Incipient safety zone can be created with distinct amounts of training data. Fig. 9 shows the results of recognizing the battery capacity accelerated decay knee point with incipient safety zone at 35 °C@1 C–1 C condition. As the amount of training data increases, the knee point cycles identified by the incipient safety zone are postponed, presenting a linear ascending relationship. Under different working conditions, the influence of the training data volume on recognizing result of the accelerated recession knee point is reported in Fig. 10. It can be seen that the accelerated attenuation point fluctuates greatly at 25 °C@1 C–1 C and 35 °C@1 C–1 C conditions, and becomes relatively stable at 45 °C@1 C–1 C condition. This may because the linearity of the height of $NE_{peak\ II}$ is discrepant during the safe operation stage. It is concluded that the recognition result of the accelerated recession point may be in advance or delayed when the incipient safety zone is established with various percentages of the total data. They have remarkable influence on the battery usage. The reliability of the battery is improved when the recognition result is in advance, and the battery will not get into the accelerated recession stage, but the economic cost of the battery is inevitably reduced. The battery will be fully utilized if the recognition result is lagging, nevertheless, the safety hazard increases, which may cause serious safety accidents.

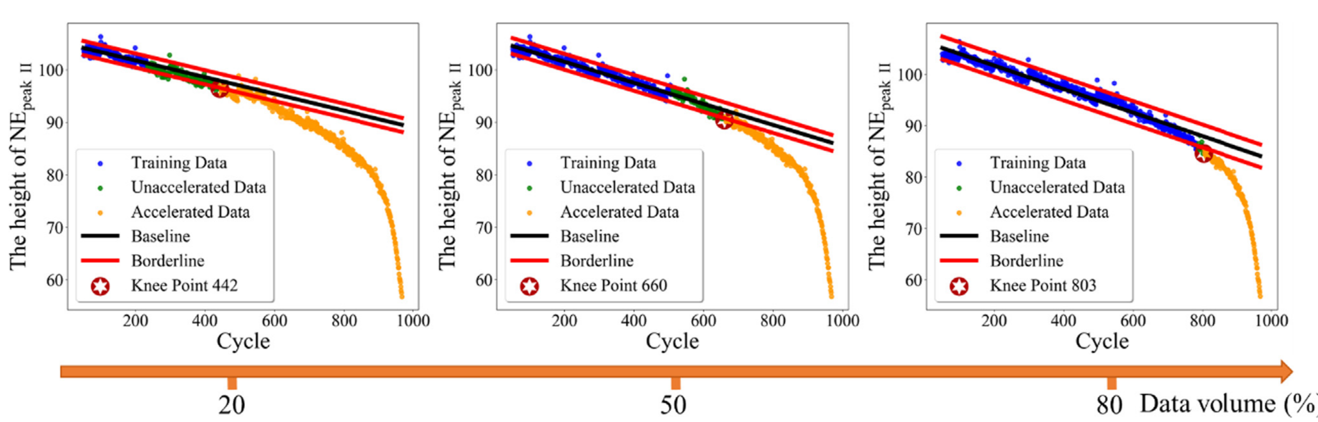

Fig. 9. The recognition results of accelerated fading knee point with incipient safety zone established by 20%, 50% and 80% data volume for the battery cycled at 35 °C@1 C–1 C condition.

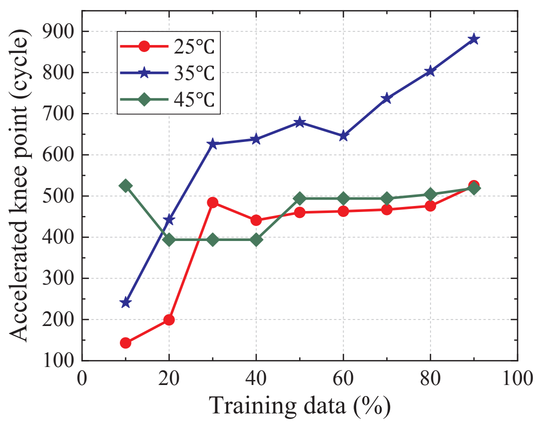

Fig. 10. The influence of the training data volume on recognizing result of the accelerated recession knee point at 25 °C@1 C–1 C, 35 °C@1 C–1 C and 45 °C@1 C–1 C conditions.

Hence, in order to eliminate the impact of training data volume on the recognition results and enhance the stability, it is momentous to update the safety boundary for the proposed method.

In this study, it is verified by experiments that the recognition results of capacity degradation knee point using proposed method appear within 90%-95% capacity range at 25 °C@1 C–1 C, 35 °C@1 C–1 C and 45 °C@1 C–1 C conditions, which can provide an early warning before the battery fails. Furthermore, using the proposed method for recognizing the sudden degradation of capacity, recognition result is effective even if the input is disturbed and has strong reliability and stability under different conditions. It is to be regretted that the proposed method is limited to the case where the attenuation of battery capacity at the safe operation stage is approximately linear. For the situation of non-linear attenuation of battery capacity at the safe operation stage, it still needs to be further research.

6. Conclusion

Nickel-Cobalt-Manganese lithium-ion batteries show an accelerated knee point in the capacity degradation process under different conditions. Based on the capacity plummeting mechanism, the paper extends the multi-index aging characterization system to the large-rate charging field and extracts effective characteristic parameters. Furthermore, a novel method for identifying the knee point of capacity decay is explored and the robustness and stability are analyzed. The main contributions are summarized as follows:

(1) The essence of capacity plummeting of Nickel-Cobalt-Manganese lithium-ion batteries is the lithium deposition of the negative electrode. The height of $NE_{peak\ II}$ reflecting the loss of available lithium ions is strongly correlated characteristic parameter and is also suitable for higher current rate condition which is validated at the current of 1 C.

(2) The developed method integrating quantile regression method and Mont Carlo simulation is used to recognize the knee point of the battery capacity decay. It is verified by experiments that the capacity degradation knee point appears within 90–95% capacity range at 25 °C, 35 °C and 45 °C conditions, which can provide an early warning before the battery fails. Recognition result is effective at different degree of the data dispersion and has adaptability to various conditions of the battery.

(3) The establishment and update of the safety zone have significant effect on the recognition results of the proposed method. It is concluded that the bandwidth calculation with the quartile and interquartile range can markedly improve the robustness and reliability of the safety zone establishment compared with two traditional methods. The incipient safety zone is established with various percentages of total data may cause the premature or hysteretic recognition result due to the change of battery degradation speed. The dynamic safety boundary determination method for the whole battery lifetime is therefore proposed to update and monitor the safety zone, making the recognition results exhibit better stability.

Acknowledgment

This work was supported by the National Key R&D Program of China [2018YFB0104001]; and National Natural Science Foundation of China [U1664255]. The authors would like to thank the members at the National Active Distribution Network Technology Research Center (NANTEC), Beijing Jiaotong University to help perform all the experiments of lithium-ion batteries mentioned in the paper.

References

[1] Andwari AM, Pesiridis A, Rajoo S, Martinez-Botas R, Esfahanian V. A review of Battery Electric Vehicle technology and readiness levels. Renew Sust Energ Rev 2017;78:414–30.
[2] Liu KL, Li K, Peng Q, Zhang C. A brief review on key technologies in the battery management system of electric vehicles. Front Mech Eng-Prc 2019;14:47–64.
[3] Zhao XR, Wang JX, Dong XT, Liu GX, Yu WS, Wang LM. Structure design and performance of LiNixCoyMn1-x-yO2 cathode materials for lithium-ion batteries: a review. J Chin Chem Soc-Taip 2014;61:1071–83.
[4] Liu S, Xiong L, He C. Long cycle life lithium ion battery with lithium nickel cobalt manganese oxide (NCM) cathode. J Power Sources 2014;261:285–91.
[5] Maheshwari A, Heck M, Santarelli M. Cycle aging studies of lithium nickel manganese cobalt oxide-based batteries using electrochemical impedance spectroscopy. Electrochim Acta 2018;273:335–48.
[6] Bacha TC, Schusterb SF, Fledera E, Müllera J, Brandb MJ, Lorrmanna H, et al. Nonlinear aging of cylindrical lithium ion cells linked to heterogeneous compression. J Storage Mater 2016;5:212–23.
[7] Yang LJ, Cheng XQ, Ma YL, Lou SF, Cui YZ, Guan T, et al. Changing of SEI film and electrochemical properties about MCMB electrodes during long-term charge/discharge cycles. J Electrochem Soc 2013;160:A2093–9.
[8] Yang XG, Leng YJ, Zhang GS, Ge SH, Wang CY. Modeling of lithium plating induced aging of lithium-ion batteries: transition from linear to nonlinear aging. J Power Sources 2017;360:28–40.
[9] Ecker M, Nieto N, K?bitz S, Schmalstieg J, Blanke H, Warnecke A, Sauer DU. Calendar and cycle life study of Li(NiMnCo)O2-based 18650 lithium-ion batteries. J Power Sour 248 (2014) 839–851.
[10] Wang J, Purewal J, Liu P, Hicks-Garner J, Soukazian S, Sherman E, et al. Degradation of lithium ion batteries employing graphite negatives and nickel-cobalt-manganese oxide plus spinel manganese oxide positives: Part 1, aging mechanisms and life estimation. J Power Sources 2014;269:937–48.
[11] Ouyang MG, Chu ZY, Lu LG, Li JQ, Han XB, Feng XN, et al. Low temperature aging mechanism identification and lithium deposition in a large format lithium iron phosphate battery for different charge profiles. J Power Sources 2015;286:309–20.
[12] Schuster SF, Bach T, Fleder E, Müller J, Brand M, Sextl G, et al. Nonlinear aging characteristics of lithium-ion cells under different operational conditions. J Storage Mater 2015;1:44–53.
[13] Klett M, Eriksson R, Groot J, Svens P, Hogstrom KC, Lindstrom RW, et al. Non-uniform aging of cycled commercial $LiFePO_4$//graphite cylindrical cells revealed by post-mortem analysis. J Power Sources 2014;257:126–37.
[14] Yang LJ, Cheng XQ, Gao YZ, Ma YL, Zuo PJ, Du CY, et al. Lithium deposition on graphite anode during long-term cycles and the effect on capacity loss. Rsc Adv 2014;4:26335–41.
[15] Sarasketa-Zabala E, Aguesse F, Villarreal I, Rodriguez-Martinez LM, Lopez CM, Kubiak P. Understanding lithium inventory loss and sudden performance fade in cylindrical cells during cycling with deep-discharge steps. J Phys Chem C 2015;119:896–906.
[16] Ma XW, Harlow JE, Li J, Ma L, Hall DS, Buteau S, et al. Hindering rollover failure of Li[Ni0.5Mn0.3Co0.2]O-2/graphite pouch cells during long-term cycling. J Electrochem Soc 2019;166:A711–24.
[17] Tang SJ, Yu CQ, Wang X, Guo XS, Si XS. Remaining useful life prediction of lithium-ion batteries based on the wiener process with measurement error. Energies 2014;7:520–47.
[18] Ramadesigan V, Chen KJ, Burns NA, Boovaragavan V, Braatz RD, Subramanian VR. Parameter estimation and capacity fade analysis of lithium-ion batteries using reformulated models. J Electrochem Soc 2011;158:A1048–54.
[19] Safari M, Delacourt C. Mathematical modeling of lithium iron phosphate electrode: galvanostatic charge/discharge and path dependence. J Electrochem Soc 2011;158:A63–73.
[20] Zhang LJ, Mu ZQ, Sun CY. Remaining useful life prediction for lithium-ion batteries based on exponential model and particle filter. IEEE Access 2018;6:17729–40.
[21] Guha A, Patra A. State of health estimation of lithium-ion batteries using capacity fade and internal resistance growth models. Ieee T Transp Electr 2018;4:135–46.
[22] Zhang H, Miao Q, Zhang X, Liu Z. An improved unscented particle filter approach for lithium-ion battery remaining useful life prediction. Microelectron Reliab 2018;81:288–98.
[23] Zhang X, Miao Q, Liu Z. Remaining useful life prediction of lithium-ion battery

using an improved UPF method based on MCMC. Microelectron Reliab 2017;75:288–95.
[24] Ng SSY, Xing Y, Tsui KL. A naive Bayes model for robust remaining useful life prediction of lithium-ion battery. Appl Energ 2014;118:114–23.
[25] Mishra M, Martinsson J, Rantatalo M, Goebel K. Bayesian hierarchical model-based prognostics for lithium-ion batteries. Reliab Eng Syst Saf 2018;172:25–35.
[26] VanDerHorn E, Mahadevan S. Bayesian model updating with summarized statistical and reliability data. Reliab Eng Syst Saf 2018;172:12–24.
[27] Yang D, Zhang X, Pan R, Wang Y, Chen Z. A novel Gaussian process regression model for state-of-health estimation of lithium-ion battery using charging curve. J Power Sources 2018;384:387–95.
[28] Wang D, Zhao Y, Yang F, Tsui K-L. Nonlinear-drifted Brownian motion with multiple hidden states for remaining useful life prediction of rechargeable batteries. Mech Syst Sig Process 2017;93:531–44.
[29] Li X, Ding Q, Sun J-Q. Remaining useful life estimation in prognostics using deep convolution neural networks. Reliab Eng Syst Saf 2018;172:1–11.
[30] Patil MA, Tagade P, Hariharan KS, Kolake SM, Song T, Yeo T, et al. A novel multistage Support Vector Machine based approach for Li ion battery remaining useful life estimation. Appl Energ 2015;159:285–97.
[31] Wei J, Dong G, Chen Z. Remaining useful life prediction and state of health diagnosis for lithium-ion batteries using particle filter and support vector regression. Ieee T Ind Electron 2018;65:5634–43.
[32] Zhang Y, Xiong R, He H, Pecht M. Lithium-ion battery remaining useful life prediction with Box-Cox transformation and Monte Carlo simulation. IEEE T Ind Electron 2018:1.
[33] Cai YS, Yang L, Deng ZW, Zhao XW, Deng H. Online identification of lithium-ion battery state-of-health based on fast wavelet transform and cross D-Markov machine. Energy 2018;147:621–35.
[34] Tao L, Lu C, Yang C. Battery capacity degradation prediction using similarity recognition based on modified dynamic time warping. Struct Control Health Monit 2018;25:e2024.
[35] Gao Y, Jiang J, Zhang C, Zhang W, Jiang Y. Aging mechanisms under different state-of-charge ranges and the multi-indicators system of state-of-health for lithium-ion battery with $Li(NiMnCo)O_2$ cathode. J Power Sources 2018;400:641–51.
[36] Gao Y, Yang S, Jiang J, Zhang C, Zhang W, Zhou X. The mechanism and characterization of accelerated capacity deterioration for lithium-ion battery with Li (NiMnCo) O_2 cathode. J Electrochem Soc 2019;166:A1623–35.
[37] Sherwood B, Wang L. Partially linear additive quantile regression in ultra-high dimension. Ann Stat 2016;44:288–317.
[38] Feng K, Lu Z, Pang C, Yun W. An efficient computational method of a moment-independent importance measure using quantile regression. Mech Syst Sig Process 2018;109:235–46.
[39] Rousseeuw PJ, Christophe C. Explicit scale estimators with high breakdown point, L1-Statistical analysis and related methods 1 (1992) 77–92.